

NLO QCD CORRECTIONS TO $WZJJ$ PRODUCTION AT THE LHC

Francisco Campanario¹, Matthias Kerner², Le Duc Ninh^{2a} and Dieter Zeppenfeld²

¹*Theory Division, IFIC, University of Valencia-CSIC, E-46980 Paterna, Valencia, Spain.*

²*Institute for Theoretical Physics, KIT, 76128 Karlsruhe, Germany.*

We present a summary of the first calculation of NLO QCD corrections to $W^\pm Zjj$ production with leptonic decays at the LHC. Our results show that the next-to-leading order corrections reduce significantly the scale uncertainties.

1 Introduction

The study of di-boson production in association with two jets at the LHC is important not only as a background to many physics searches, but also, as a signal since it is sensitive to the quartic gauge couplings of the Standard Model (SM) and the four-vector-boson scatterings of the type $VV \rightarrow VV$ where the initial gauge bosons are radiated from the incoming (anti-)quarks. At leading order (LO), there are three different production mechanisms. The vector boson fusion mechanism of the order $\mathcal{O}(\alpha^6)$ includes in particular the electroweak (EW) gauge-boson scattering and it has been studied at NLO QCD in Refs. ^{1,2,3,4,5}. In addition, the production of three EW gauge bosons, with one off-shell gauge boson decaying into a quark-antiquark pair, is a second source of $VVjj$ events at order $\mathcal{O}(\alpha^6)$ and will be available at NLO QCD with leptonic decays via the VBFNLO program ^{6,7}.

Finally, there are QCD contributions of the order $\mathcal{O}(\alpha_s^2\alpha^4)$. The NLO QCD corrections to this mechanism have been calculated for the W^+W^-jj production in Refs. ^{8,9}, for the W^+W^+jj case in Ref. ¹⁰ and recently in Ref. ¹¹ for the $\gamma\gamma jj$ and in Ref. ¹² for the $W^\pm Zjj$ channels. Indeed, the last processes with one undetected lepton are the main backgrounds to the same-charge W^+W^+jj/W^-W^-jj observation at the LHC.

Since the above three production modes peak in different regions of phase space, and because of their largely orthogonal color structures, interference effects between these modes are generally unimportant and can be neglected in most applications.

In the following, we consider the QCD induced $W^\pm Zjj$ production modes within the SM.

2 Calculation

In this section, we define the problem and summarize our calculational method. The processes are

$$\begin{aligned} pp &\rightarrow e^+ \nu_e \mu^+ \mu^- jj + X, \\ pp &\rightarrow e^- \bar{\nu}_e \mu^+ \mu^- jj + X, \end{aligned} \tag{1}$$

^aSpeaker

where $p, j = g, u, d, c, s$ and the corresponding anti-quarks. The subprocesses with t, b are neglected since their contributions are very small. At LO, only the QCD mechanism as illustrated in Fig. 1 is included. The dominant contribution comes from the diagrams where both W^\pm and

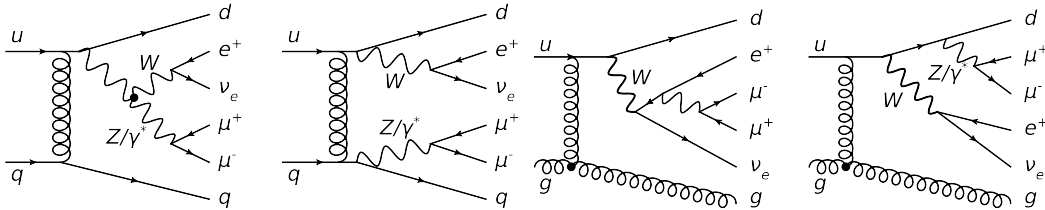


Figure 1: Representative tree-level Feynman diagrams.

Z can be simultaneously on-shell. This is why we refer to the processes Eq. (1) as $W^\pm Z jj$ production. However, the sub-dominant diagrams with one resonating gauge boson are also included, hence the total amplitudes are QCD and EW gauge invariant. The challenge is then to calculate the NLO QCD corrections to get theoretical prediction at order $\mathcal{O}(\alpha_s^3 \alpha^4)$.

At NLO, there are the virtual and the real corrections as shown in Fig. 2. There are 90 and

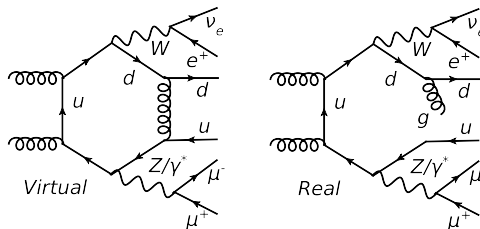


Figure 2: Representative virtual and real-gluon emission Feynman diagrams.

146 subprocesses for the LO and real-emission contributions, respectively. Both the virtual and real corrections are, apart from the UV divergences in the virtual amplitude which are removed by the renormalization of α_s , separately infrared divergent. These divergences cancel in the sum for infrared-safe observables such as the inclusive cross section and jet distributions. We use the dimensional regularization method¹³ to regularize the UV and the infrared divergences and apply the Catani-Seymour dipole subtraction algorithm¹⁴ to combine the virtual and the real contributions. The most difficult part of the calculation is computing the 2-quark-2-gluon virtual amplitudes with up to six-point rank-five one-loop tensor integrals. There are 84 six-point diagrams for each of seven independent subprocesses. The 4-quark group is much easier with only 12 hexagons for the most complicated subprocesses with same-generation quarks. Given the complexity of the calculation, we have implemented two independent codes. Details of the implementation and cross checks are given in Ref. 12.

3 Numerical results

As input parameters, we choose the following inclusive cuts. For leptons:

$$p_{T,\ell} \geq 20 \text{ GeV}, \quad |y_\ell| \leq 2.5, \quad E_{T,\text{miss}} \geq 30 \text{ GeV}, \quad m_{\ell+\ell^-} \geq 15 \text{ GeV}, \quad (2)$$

where the last cut is for any pair of opposite-charge leptons. For jets, we use the anti- k_t algorithm¹⁵ with radius $R = 0.4$ and

$$p_{T,\text{jet}} \geq 20 \text{ GeV}, \quad |y_{\text{jet}}| \leq 4.5. \quad (3)$$

We also impose a requirement on the lepton-lepton and lepton-jet separation in the azimuthal angle-rapidity plane $\Delta R_{\ell(\ell,j)} \geq 0.4$, where only jets passing the above cuts are considered. As

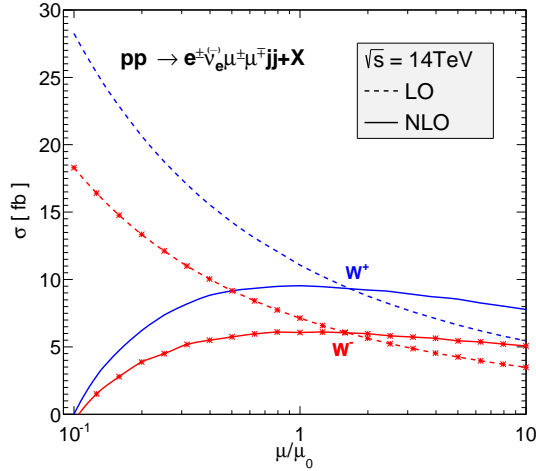


Figure 3: Scale dependence of the LO and NLO cross sections at the LHC. The curves with and without stars are for $W^- Zjj$ and $W^+ Zjj$ productions, respectively.

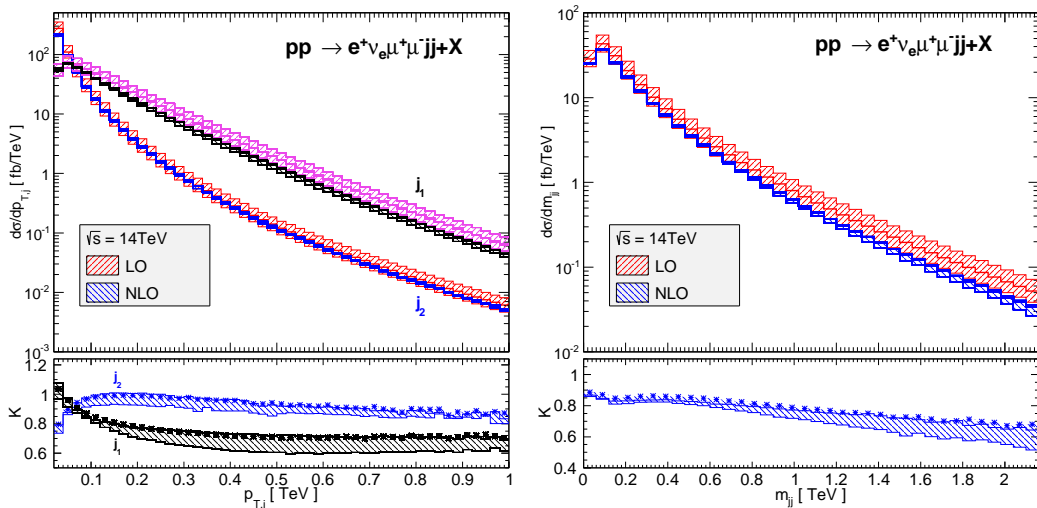


Figure 4: Differential cross sections and K -factors for the transverse momenta (left) and the invariant mass (right) of the two hardest jets. The bands describe $\mu_0/2 \leq \mu_F = \mu_R \leq 2\mu_0$ variations. The K -factor bands are due to the scale variations of the NLO results, with respect to $\sigma_{\text{LO}}(\mu_0)$. The curves with stars in the lower panels are for the central scale, while the two solid lines correspond to $\mu_F = \mu_R = 2\mu_0$ and $\mu_0/2$.

the central value for the factorization and renormalization scales, we choose

$$\mu_F = \mu_R = \mu_0 = \left(\sum_{\text{jet}} p_{T,\text{jet}} + \sqrt{p_{T,W}^2 + m_W^2} + \sqrt{p_{T,Z}^2 + m_Z^2} \right) / 2, \quad (4)$$

where $p_{T,V}$ and m_V with V being W or Z are the reconstructed transverse momenta and invariant masses of the decaying bosons and the sum includes only jets passing all cuts.

In Fig. 3, we plot the cross section calculated at LO and NLO as functions of $\mu = \mu_F = \mu_R$. As expected, we observe a significant reduction in the scale dependence around the central value μ_0 when the NLO contribution is included. For both W^+ and W^- cases, the uncertainties obtained by varying $\mu_{F,R}$ by factors 1/2 and 2 around the central value are 50% at LO and 5% at NLO. At $\mu = \mu_0$, we get $\sigma_{\text{LO}} = 11.1^{+3.2}_{-2.3}$ fb ($7.1^{+2.0}_{-1.5}$ fb) and $\sigma_{\text{NLO}} = 9.5^{+0.0}_{-0.4}$ fb ($6.1^{+0.0}_{-0.3}$ fb) for the W^+ (W^-) case. By varying the two scales separately, we observe a small dependence on μ_F , while the μ_R dependence is similar to the behavior shown in Fig. 3.

The distributions of the transverse momenta and the invariant mass of the two hardest jets are shown in Fig. 4. The K -factors, defined as the ratio of the NLO to the LO results, are

shown in the lower panels. The distributions at NLO are much less sensitive to the variation of the scales than at LO. The K -factors vary from 0.6 to 1 in a large energy range. We have also studied a fixed scale choice such as $\mu_0^{\text{fix}} = 400 \text{ GeV}$ and found that the NLO inclusive cross section as a function of the scales is stable around μ_0^{fix} and is close to the LO one as well as the dynamic scale prediction. However, the transverse momentum and the invariant mass distributions become unstable at large p_T , with very small K -factors. This is because the bulk of the inclusive cross section comes from the low energy regime as shown in Fig. 4, but a fixed energy scale is not appropriate for all energy regimes. The steep increase of the K -factor for the transverse momentum distribution of the second hardest jet near 20 GeV is probably a threshold effect: the phase space for three-visible-jet events is opened up as p_{T,j_2} grows well above the cut of 20 GeV.

4 Conclusions

In this talk, we have reported on the first calculation of $W^\pm Zjj + X$ production at order $\mathcal{O}(\alpha_s^3 \alpha^4)$ and found K -factors close to one. This is a part of our project to include NLO QCD corrections to $VVjj$ production processes at the LHC in the VBFNLO program^{6,7}.

Acknowledgments

LDN would like to thank the organizers, in particular Tran Thanh Van, for the nice conference. We acknowledge the support from the Deutsche Forschungsgemeinschaft via the Sonderforschungsbereich/Transregio SFB/TR-9 Computational Particle Physics. FC is funded by a Marie Curie fellowship (PIEF-GA-2011-298960) and partially by MINECO (FPA2011-23596) and by LHCPHENONET (PITN-GA-2010-264564). MK is supported by the Graduiertenkolleg 1694 “Elementarteilchenphysik bei höchster Energie und höchster Präzision”.

References

1. B. Jager, C. Oleari, and D. Zeppenfeld, JHEP **0607**, 015 (2006), hep-ph/0603177.
2. B. Jager, C. Oleari, and D. Zeppenfeld, Phys.Rev. **D73**, 113006 (2006), hep-ph/0604200.
3. B. Jager, C. Oleari, and D. Zeppenfeld, Phys.Rev. **D80**, 034022 (2009), arXiv:0907.0580.
4. A. Denner, L. Hosekova, and S. Kallweit, Phys.Rev. **D86**, 114014 (2012), arXiv:1209.2389.
5. F. Campanario, N. Kaiser, and D. Zeppenfeld, (2013), 1309.7259.
6. K. Arnold *et al.*, Comput.Phys.Commun. **180**, 1661 (2009), 0811.4559.
7. K. Arnold *et al.*, (2012), arXiv:1207.4975.
8. T. Melia, K. Melnikov, R. Rontsch, and G. Zanderighi, Phys.Rev. **D83**, 114043 (2011), arXiv:1104.2327.
9. N. Greiner *et al.*, Phys.Lett. **B713**, 277 (2012), arXiv:1202.6004.
10. T. Melia, K. Melnikov, R. Rontsch, and G. Zanderighi, JHEP **1012**, 053 (2010), arXiv:1007.5313.
11. T. Gehrmann, N. Greiner, and G. Heinrich, (2013), 1308.3660.
12. F. Campanario, M. Kerner, L. D. Ninh, and D. Zeppenfeld, Phys. Rev. Lett. **111**, 052003 (2013), arXiv:1305.1623.
13. G. 't Hooft and M. Veltman, Nucl.Phys. **B44**, 189 (1972).
14. S. Catani and M. Seymour, Nucl.Phys. **B485**, 291 (1997), hep-ph/9605323.
15. M. Cacciari, G. P. Salam, and G. Soyez, JHEP **0804**, 063 (2008), arXiv:0802.1189.